

# AN ALGORITHM FOR PLANAR FOUR-BAR MOTION GENERATION WITH OPTIMIZATION

PETER J. MARTIN<sup>a</sup>, KEVIN RUSSELL<sup>a,\*</sup>, WEN-TZONG LEE<sup>b</sup>, RAJ S. SODHI<sup>c</sup>

<sup>a</sup>*Armaments Engineering and Technology Center,  
US Army Research, Development and Engineering Center,  
Picatinny Arsenal, NJ 07806-5000, U.S.A*

\*Contact: kevin.russell1@us.army.mil

<sup>b</sup>*Department of Information Management, Leader University  
Taiana, 70970, TAIWAN*

<sup>c</sup>*Department of Mechanical Engineering, New Jersey Institute of Technology,  
Newark, NJ 07102-1982, U.S.A*

Received May 2007, Accepted November 2007

No. 07-CSME-27, E.I.C. Accession 2996

---

## ABSTRACT

A set of fixed and moving pivot loci can represent an infinite number of planar four-bar motion generator solutions for a given series of prescribed rigid-body poses. Unfortunately, given the vast number of possible mechanical solutions in a set of fixed and moving pivot loci, it is difficult for designers to arbitrarily select a fixed and moving pivot loci solution that ensures full link rotatability, produces feasible transmission angles and is a compact design. This work presents an algorithm for selecting planar four-bar motion generators with respect to Grashof conditions, transmission angle conditions and having the minimum perimeter value. This algorithm has been codified into MathCAD for enhanced analysis capabilities and ease of use. The example in this work demonstrates the synthesis of a compact planar, four-bar crank-rocker motion generator with feasible transmission angles.

---

## UN ALGORITHME POUR LA GÉNÉRATION DE MOUVEMENT PLANAIRE À QUATRE BARRES AVEC OPTIMISATION

### RÉSUMÉ

Une série de points pivots fixes et mobiles peut représenter un nombre infini de solutions de générateur de mouvement planaire à quatre barres pour une série donnée de poses à corps rigide. Malheureusement, étant donné le grand nombre de solutions mécaniques possibles dans une série de points de pivots fixes et mobiles, il est difficile pour les concepteurs de sélectionner arbitrairement une solution de points pivots fixes et mobiles qui assure la rotatabilité à lien complet et produit des angles de transmission réalisables, en plus d'être un design compact. Cet article présente un algorithme pour sélectionner des générateurs de mouvement planaire à quatre barres en ce qui a trait conditions Grashof et de l'angle de transmission conditions, et pour avoir une valeur de périmètre minimale. Cet algorithme a été codifié en un Mathcad pour améliorer les capacités d'analyse et faciliter l'usage. L'exemple offert dans ce travail démontre la synthèse d'un générateur de mouvement compact de manivelle agitateur à quatre barres avec des angles de transmission réalisables.

## 1. INTRODUCTION

### 1.1 Background and Objective

The objective in kinematic motion generation is to determine the mechanism parameters required to approximate or precisely achieve a series of prescribed rigid-body poses. Motion generation methods, specifically those that generate fixed and moving pivot loci produce an infinite number of solutions for a prescribed series of rigid-body poses. In other words, the user can select a mechanism solution from a potentially infinite array of possible mechanism solutions. Although all of these solutions may be kinematically feasible, some of them may not represent practical engineering solutions. For example, some mechanisms may produce undesired transmission angles, require large workspaces or not ensure full link rotatability.

One possible approach to employ motion generation (using fixed and moving pivot loci as input) while adhering to specific mechanism design conditions and constraints is through a search and selection algorithm. This work presents an algorithm for selecting planar four-bar motion generators with respect to Grashof conditions, transmission angle conditions and having the minimal perimeter value. This algorithm has been codified into MathCAD for enhanced analysis capabilities.

### 1.2 Literature Review

Mechanism synthesis with optimization includes the work of Yao and Angeles [1] who apply the contour method in the approximate synthesis of planar linkages for rigid-body guidance. Cabrera et al [2] considers solution methods for the optimal synthesis of planar mechanisms. Cossalter et al [3] presented a numerical method for optimum synthesis of planar mechanisms for motion, path and function generation. The work of Krishnamurty and Turcic [4] applies non-linear goal programming for the optimal synthesis of planar mechanisms. The work of Akhras and Angeles [5] considers unconstrained non-linear least-square techniques in the optimization of planar linkages for rigid-body guidance. Sandgren's [6] work proposes a design tree structure for the optimization of mechanisms that considers both geometric and topological change. Khare and Dave [7] presented a procedure for the synthesis of planar four-bar double-rocker mechanisms for coordinating the prescribed extreme positions. The work of Da Lio et al [8] deals with the use of natural coordinates for the synthesis of mechanisms using optimization methods. A gradient-based optimization approach for path synthesis problems was proposed by Sancibrian et al [9] and a global optimum obtaining problem in approximate path synthesis of linkages was considered by Marín and González [10]. The work of Avilés et al [11] presents a method for the optimum synthesis of planar mechanisms with lower pairs and a configuration of any type. Vasiliu and Yannou [12] proposed a method to synthesize the dimensions of a planar path generator. Rao [13] applies geometric programming to the synthesis of planar four-bar function generators using optimization based on neural networks and spherical mechanisms with minimum structural error. The kinematic analysis and design optimization of spatial parallel manipulators were considered in the works of Tsai and Joshi [14] and Carretero et al [15]. Hong and Erdman [16] introduced a new application Burmester curves for adjustable linkages. In the work of Arsenault and Boudreau [17], planar parallel mechanisms are synthesized with respect to workspace, dexterity, stiffness and singularity avoidance. In the work of Smaili et al [18] a tabu-gradient search algorithm is incorporated for the optimum synthesis of linkages.

## 2. PLANAR RIGID-BODY GUIDANCE

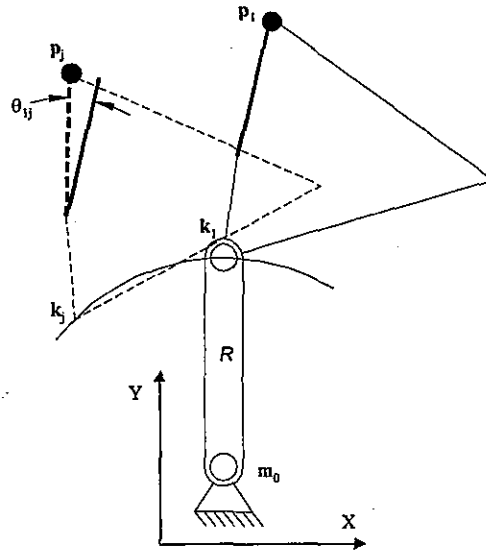


Fig. 1. Four-bar mechanism dyad with coupler point  $p$  and orientation angle  $\theta$

Figure 1 illustrates a dyad of a planar four-bar mechanism in position 1 and position "j". The displacement of the rigid-body between the 1<sup>st</sup> and j<sup>th</sup> positions is determined by the displacement of rigid-body point  $p_1$  and the simultaneous rigid-body angular displacement  $\theta_{ij}$ . Given a general fixed pivot  $m_0$  and a moving pivot  $k_1$ , the constant length condition in Eqn. (1) [19,20] must be satisfied when synthesizing the crank and follower links of the planar four-bar mechanism.

$$(\mathbf{k}_j - \mathbf{m}_0)^T (\mathbf{k}_j - \mathbf{m}_0) = (\mathbf{k}_1 - \mathbf{m}_0)^T (\mathbf{k}_1 - \mathbf{m}_0) \quad j = 2,3,4,5 \quad (1)$$

where

$$\mathbf{m}_0 = (m_{0x}, m_{0y}, 1), \quad \mathbf{k}_1 = (k_{1x}, k_{1y}, 1) \quad \mathbf{k}_j = [\mathbf{D}_{1j}] \mathbf{k}_1$$

and

$$[\mathbf{D}_{1j}] = \begin{bmatrix} \cos\theta_{ij} & -\sin\theta_{ij} & p_{jx} - p_{1x}\cos\theta_{ij} + p_{1y}\sin\theta_{ij} \\ \sin\theta_{ij} & \cos\theta_{ij} & p_{jy} - p_{1x}\sin\theta_{ij} - p_{1y}\cos\theta_{ij} \\ 0 & 0 & 1 \end{bmatrix} \quad (2)$$

Eqn. (2) is the rigid-body displacement matrix from position 1 to position j. Eqn. (1) is rewritten as Eqn. (3) where the variable  $R$  is the scalar link length.

$$(\mathbf{k}_j - \mathbf{m}_0)^T (\mathbf{k}_j - \mathbf{m}_0) = R^2 \quad j = 2,3,4,5 \quad (3)$$

The planar four-bar dyad in Fig. 1 has a maximum of five unknown variables ( $m_{0x}$ ,  $m_{0y}$ ,  $k_{1x}$ ,  $k_{1y}$  and  $R$ ). Given four prescribed rigid-body poses (from five prescribed rigid-body positions) Eqns. (4) through (7) can be used to calculate four of the five unknown variables.

$$([\mathbf{D}_{12}] \mathbf{k}_1 - \mathbf{m}_0)^T ([\mathbf{D}_{12}] \mathbf{k}_1 - \mathbf{m}_0) - R^2 = 0 \quad (4)$$

$$([\mathbf{D}_{13}] \mathbf{k}_1 - \mathbf{m}_0)^T ([\mathbf{D}_{13}] \mathbf{k}_1 - \mathbf{m}_0) - R^2 = 0 \quad (5)$$

$$([\mathbf{D}_{14}] \mathbf{k}_1 - \mathbf{m}_0)^T ([\mathbf{D}_{14}] \mathbf{k}_1 - \mathbf{m}_0) - R^2 = 0 \quad (6)$$

$$([\mathbf{D}_{15}] \mathbf{k}_1 - \mathbf{m}_0)^T ([\mathbf{D}_{15}] \mathbf{k}_1 - \mathbf{m}_0) - R^2 = 0 \quad (7)$$

Because one of the five unknown dyad variables is specified using Eqns. (4) through (7), the user is free to specify a range of values for any particular variable and calculate the solutions corresponding to the

prescribed range. For example, the user can specify a range for variable  $m_{0x}$  and calculate  $m_{0y}$ ,  $k_{1x}$ ,  $k_{1y}$  and  $R$  for each  $m_{0x}$  value in the specified range of  $m_{0x}$ . These solutions include a fixed pivot locus ( $\mathbf{m}_0$ ) and a moving pivot locus ( $\mathbf{k}_1$ ) of planar four-bar mechanism solutions for the prescribed rigid-body poses. Figure 2 illustrates fixed and moving pivot loci produced (given four prescribed arbitrary rigid-body poses) using the method previously described.

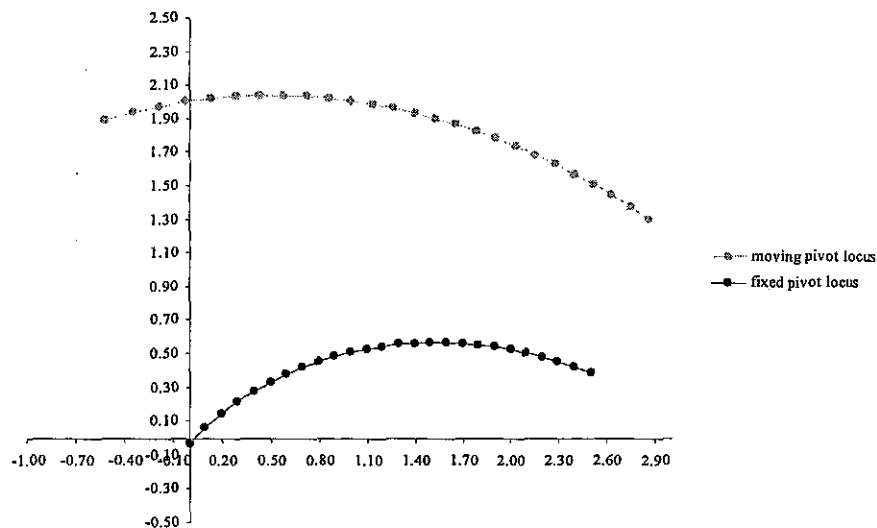


Fig. 2. Calculated fixed and moving pivot loci

### 3. GRASHOF CRITERIA, TRANSMISSION ANGLE AND MECHANISM PERIMETER CRITERIA

#### 3.1 Methodology

Full link rotatability is a particularly practical design characteristic for planar four-bar mechanisms—especially when the crank link is driven by a drive system that rotates continuously. Grashof criteria predict the rotation behavior (or rotatability) of a four-bar linkage's inversions based on its link lengths. Table 1 includes the five Grashof classifications for planar four-bar mechanisms. In this table, variables  $L_{min}$ ,  $L_{max}$ ,  $L_a$  and  $L_b$  represent the shortest link length, longest link length and intermediate link lengths respectively. With the exception of the Grashof triple rocker, all other Grashof classifications have full link rotatability.

An additional practical design characteristic for planar four-bar mechanisms is that it produces feasible transmission angles. The transmission angle is the angle between the coupler link and the follower link. A transmission angle of  $90^\circ$  is ideal while angles of  $0^\circ$  and  $180^\circ$  result in maximum joint loading in the mechanism and subsequently maximum joint wear.

Another practical design characteristic for planar four-bar mechanisms is compactness. In this work, a compact mechanism is defined as one in which the sum of the crank, coupler, follower and ground lengths (or the mechanism perimeter) is the smallest possible. In general, compact mechanisms produce smaller workspaces and are more structurally sound than four-bar mechanisms with larger perimeters.

**Table 1.** Planar four-bar mechanism Grashof classifications

| Type of mechanism | Shortest link | Link length Relationships       |
|-------------------|---------------|---------------------------------|
| Crank-Rocker      | Crank         | $L_{max} + L_{min} < L_a + L_b$ |
| Drag Link         | Ground        | $L_{max} + L_{min} < L_a + L_b$ |
| Double-Rocker     | Coupler       | $L_{max} + L_{min} < L_a + L_b$ |
| Change Point      | Any           | $L_{max} + L_{min} = L_a + L_b$ |
| Triple Rocker     | Any           | $L_{max} + L_{min} > L_a + L_b$ |

### 3.2 Algorithm

Figure 3 illustrates a diagram of the optimization algorithm. As this figure illustrates, the generated fixed and moving pivot loci are the algorithm input and the parameters of an optimized motion generator are the algorithm output.

Block 1 in Fig. 3 involves the calculation of every mechanism solution for the given fixed and moving pivot loci. Since numerically-generated fixed and moving pivot loci can have an indefinite number of data points, the number of discrete loci data points to include is at the discretion of the user. Appendix A1 includes the MathCAD commands to calculate lengths of the crank, coupler, follower and ground links for every mechanism solution for the given fixed and moving pivot loci points.

Block 2 in Fig. 3 involves the selection (from among the possible mechanism solutions produced in block 1) of all mechanism solutions that satisfy user-defined minimum and maximum transmission angle conditions. To determine mechanism solutions with feasible transmission angles, the transmission angles of all mechanism solutions from block 1 are calculated for a prescribed crank rotation range. Appendix A2 includes the MathCAD commands for transmission angle calculation and selection of mechanism solutions with feasible transmission angles.

Block 3 in Fig. 3 involves the selection of all mechanism solutions of a particular Grashof classification from among the possible solutions produced in block 2. Table 1 includes all of the Grashof mechanism classifications and conditions. The example in this work demonstrates the synthesis of a compact planar, four-bar crank-rocker motion generator. Appendix A3 includes the MathCAD commands to select Grashof crank-rocker solutions.

Block 4 in Fig. 3 involves the selection of the mechanism solutions from among the possible solutions produced in block 3 with the minimum perimeter. A minimum perimeter condition can help improve the efficiency in selecting compact four-bar motion generator designs. In general, compact mechanisms produce smaller workspaces and are more structurally sound than four-bar mechanisms with larger perimeters. Appendix A4 includes the MathCAD commands to locate the most compact Grashof crank-rocker solution.

Block 5 in Fig. 3 involves the determination of the dimensional parameters of the compact planar four-bar (crank-rocker) motion generator selected in block 4. Such parameters include the coordinates of the fixed pivots and moving pivots of the optimized planar four-bar mechanism. The joints of a planar four-bar motion generator are represented by two pairs of fixed and moving pivot points (two  $m-k_1$  pairs) from the associated fixed and moving pivot loci. Appendix A5 includes the MathCAD commands to locate the coordinates of the fixed and moving pivots of the compact Grashof crank-rocker solution.

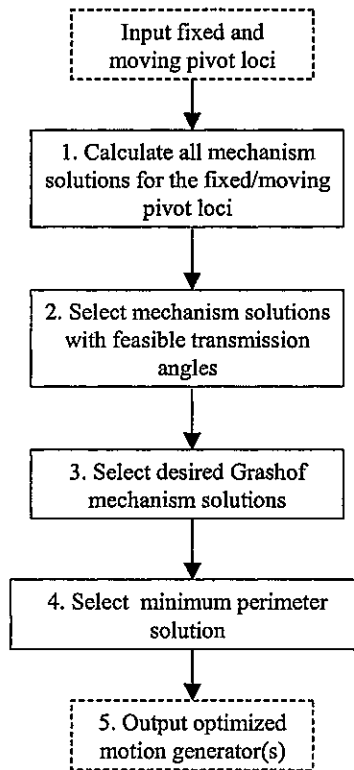


Fig. 3. Motion generation with optimization algorithm diagram

#### 4. EXAMPLE

Five prescribed rigid-body poses are included in Table 2. For this motion generation application, a Grashof crank-rocker with a minimized perimeter angles between  $40^\circ$  and  $140^\circ$  is a satisfactory solution. Using the numerical fixed and moving pivot curve generation method in Section 2 with the following prescribed range and initial guesses:

$$m_{ox} = -0.60, -0.50 \dots 2.30, \quad m_{oy} = -0.5, \quad \mathbf{k}_1 = (0.5, 1.0), \quad R = 2$$

the fixed and moving pivot loci illustrated in Fig. 4 were generated.

From the fixed and moving pivot loci in Fig. 4, the line plot in Fig. 5 illustrates all possible crank and follower length solutions and the surface plots in Fig. 6 illustrate all possible coupler and ground length solutions. Although all of these solutions are planar four-bar motion generators that will approximate the prescribed rigid-body poses, an acceptable mechanism solution in this example is a compact Grashof crank-rocker with feasible transmission angles.

In Fig. 4, there are 30 data points each for the fixed and moving pivot loci. Each fixed pivot locus point ( $\mathbf{m}_0$ ) has a corresponding moving pivot locus point ( $\mathbf{k}_1$ ) or vice-versa. There are 30  $\mathbf{m}_0$ - $\mathbf{k}_1$  pairs that represent crank or follower links with the given prescribed range for  $m_{ox}$ . In Fig. 5, each  $\mathbf{m}_0$ - $\mathbf{k}_1$  pair is assigned a cell number (for use in MathCAD) and the scalar magnitude of each  $\mathbf{m}_0$ - $\mathbf{k}_1$  pair is the length of the crank/follower link. If any two  $\mathbf{m}_0$ - $\mathbf{k}_1$  pairs are considered, the scalar magnitudes between the two  $\mathbf{k}_1$  and  $\mathbf{m}_0$  points are the lengths of the coupler and ground links respectively. Fig. 6 illustrates every possible coupler and ground length solution for the prescribed rigid-body poses. These surface plots are the result of measuring the scalar coupler and ground lengths from every possible combination of any two  $\mathbf{m}_0$ - $\mathbf{k}_1$  pairs in Fig. 4. To select a mechanism solution that meets all of the stated design requirements from this number of possible solutions without a search and selection algorithm that incorporates the stated design requirements is not a simple task.

Fig. 7 illustrates the compact Grashof crank-rocker motion generator solution produced from the algorithm included in the Appendix and Fig. 8 illustrates the transmission angles achieved by this mechanism. Appendix A5 produced the two  $\mathbf{m}_0\text{-}\mathbf{k}_1$  pairs that the four-bar motion generator in Fig. 7 is comprised of. The left-side  $\mathbf{m}_0\text{-}\mathbf{k}_1$  pair (or crank link) in Fig. 7 has coordinates of  $\mathbf{m}_0=(-0.6, -0.6527)$  and  $\mathbf{k}_1=(-0.5425, 0.1305)$ . The right-side  $\mathbf{m}_0\text{-}\mathbf{k}_1$  pair (or follower link) in Fig. 7 has coordinates of  $\mathbf{m}_0=(2.1, -0.5492)$  and  $\mathbf{k}_1=(2.1047, 0.7476)$ . The rigid-body poses achieved by the compact crank-rocker motion generator are included in Table 3.

**Table 2.** Prescribed rigid-body poses

| $p_x, p_y$      | $\theta$ [deg.] |
|-----------------|-----------------|
| 1.0011, 1.8729  |                 |
| 0.6555, 1.8167  | 0.2378          |
| 0.3324, 1.6679  | 1.6780          |
| 0.0593, 1.4529  | 4.7543          |
| -0.1561, 1.2117 | 10.3149         |

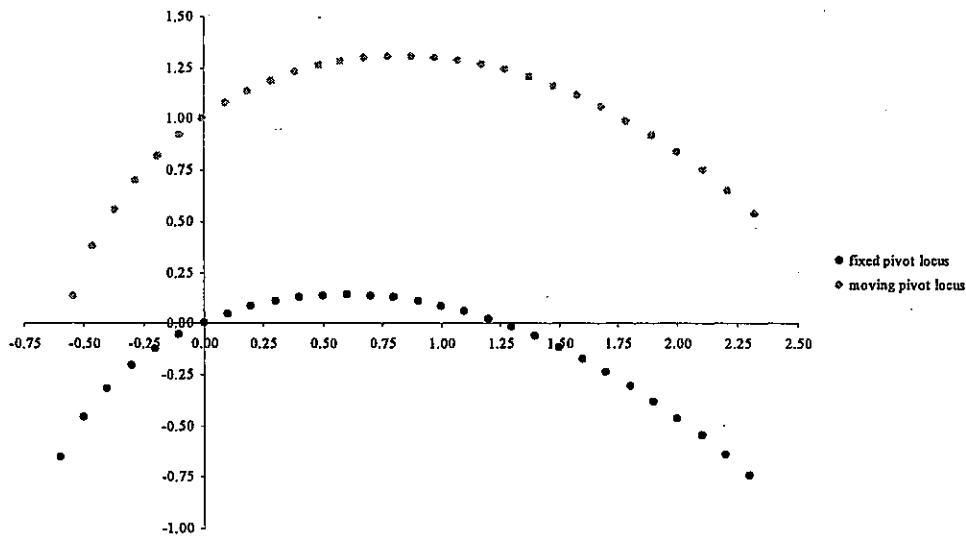


**Fig. 4.** Fixed and moving pivot loci for prescribed rigid-body poses



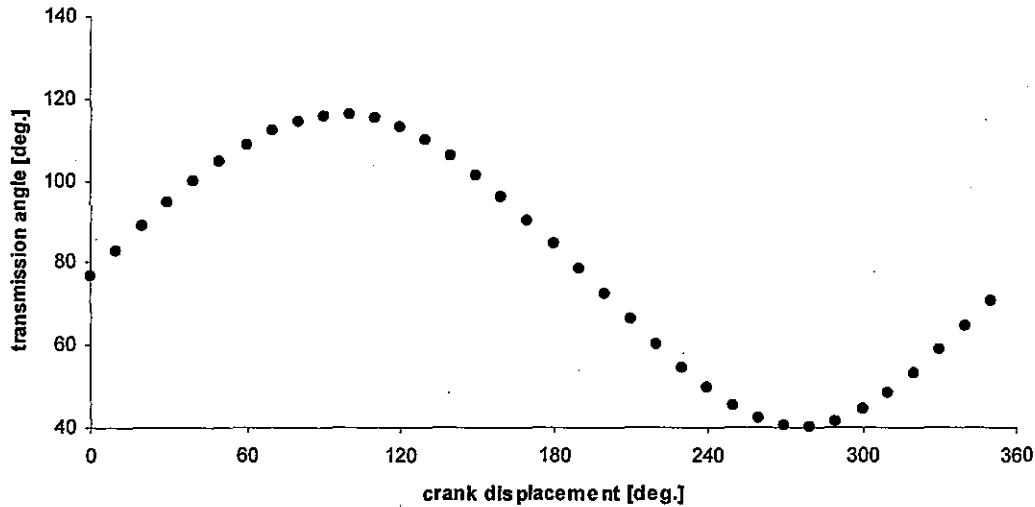


Fig. 8. Transmission angles of optimized motion generator

Table 3. Rigid-body poses by synthesized motion generator

| $p_x, p_y$      | $\theta$ [deg.] | crank disp. angle [deg.] |
|-----------------|-----------------|--------------------------|
| 1.0011, 1.8729  |                 |                          |
| 0.6541, 1.8250  | 0.1399          | 25.5000                  |
| 0.3334, 1.6777  | 1.5396          | 50.0000                  |
| 0.0552, 1.4594  | 4.6038          | 75.5000                  |
| -0.1637, 1.2143 | 10.1643         | 103.0000                 |

## 5. DISCUSSION

To account for both planar four-bar mechanism branches (two coupler and follower configurations for a given crank position or the “open” and “crossed” mechanism configurations [22]) in the algorithm, the fixed and moving pivot loci for both mechanism branches must be generated and read into the algorithm. Although the fixed reference in Eqn. (2) provides a measure order assurance, the presented algorithm includes no processes to guarantee order conformity between the prescribed and approximated rigid-body poses. Using MathCAD and AutoCAD software, all of the data calculated and measured in this work were specified to four decimal places. These software packages can calculate and measure numbers to over eight decimal places. The Grashof conditions in the secondary algorithm (Appendix A3) can be modified to enable the user to design compact motion generators of any Grashof type. In Appendix A1, the data points on the circle and center pivot curves are fed into the secondary algorithm to calculate the lengths of the crank, coupler, follower and ground link solutions. Variable “end” in this Appendix A1 denotes the total number of  $m_0-k_1$  pairs used (in the example problem, 30 pairs were used). Although a mechanism solution was down-selected from a finite number of fixed and moving pivot loci points in the example, the algorithm can accommodate an indefinite number of locus data points (particularly when the algorithm is codified on a computationally-robust platform). Due to the lack of space, an abridged version of the codified algorithm has been included in the Appendix. For the entire codified algorithm, refer to reference [21]. Although one particular numerical fixed and moving pivot loci generation method is described in this work, any fixed and moving pivot loci generation approach is applicable since the

algorithm presented by the authors requires only the discrete complex circle and center point coordinates (Fig. 4).

## 6. CONCLUSION

The algorithm presented in this work was demonstrated to be effective in down-selecting a planar four-bar motion generator solution with respect to Grashof crank-rocker criteria, minimum and maximum transmission angle constraints and having minimum mechanism perimeter given a finite set of discrete fixed and moving pivot loci data points. This algorithm was successfully codified in the mathematical analysis software MathCAD for enhanced analysis capabilities and ease of use (e.g., predefined operations for matrix manipulation).

## REFERENCES

1. J. Yao and J. Angeles, "Computation of all optimum dyads in the approximate synthesis of planar linkages for rigid-body guidance," *Mechanism and Machine Theory*, Vol. 35, No. 8, pp. 1065-1078, 2000.
2. J. A. Cabrera, A. Simon and M. Prado, "Optimal synthesis of mechanisms with genetic algorithms," *Mechanism and Machine Theory*, Vol. 37, No. 10, pp. 1165-1177, 2002.
3. V. Cossalter, A. Doria and M. Pasini, "A simple numerical approach for optimum synthesis of a class of planar mechanisms," *Mechanism and Machine Theory*, Vol. 27, No. 3, pp. 357-366, 1992.
4. S. Krishnamurty and D. A. Turcic, "Optimal synthesis of mechanisms using nonlinear goal programming techniques," *Mechanism and Machine Theory*, Vol. 27, No. 5, pp. 599-612, 1992.
5. R. Akhras and J. Angeles, "Unconstrained nonlinear least-square optimization of planar linkages for rigid-body guidance," *Mechanism and Machine Theory*, Vol. 25, No. 1, pp. 97-118, 1990.
6. E. Sandgren, "A multi-objective design tree approach for the optimization of mechanisms," *Mechanism and Machine Theory*, Vol. 25, No. 3, pp. 257-272, 1990.
7. A. K. Khare and R. K. Dave, "Optimizing 4-bar crank-rocker mechanism," *Mechanism and Machine Theory*, Vol. 14, No. 5, pp. 319-325, 1979.
8. M. Da Lio, V. Cossalter and R. Lot, "On the use of natural coordinates in optimal synthesis of mechanisms," *Mechanism and Machine Theory*, Vol. 35, No. 10, pp. 1367-1389, 2000.
9. R. Sancibrian, P. García, F. Viadero and A. Fernández, "A general procedure based on exact gradient determination in dimensional synthesis of planar mechanisms," *Mechanism and Machine Theory* (In Press).
10. F. T. S. Marín and A. P. González, "Global optimization in path synthesis based on design space reduction," *Mechanism and Machine Theory*, Vol. 38, No. 6, pp. 579-594, 2003.
11. J. V. R. Avilés, A. Hernández and E. Amezua, "Nonlinear optimization of planar linkages for kinematic syntheses," *Mechanism and Machine Theory*, Vol. 30, No. 4, pp. 501-518, 1995.

12. A. Vasiliu and B. Yannou, "Dimensional synthesis of planar mechanisms using neural networks: application to path generator linkages," *Mechanism and Machine Theory*, Vol. 36, No. 2, pp. 299-310, 2001.
13. A. C. Rao, "Synthesis of 4-bar function-generators using geometric programming," *Mechanism and Machine Theory*, Vol. 14, No. 2, pp. 141-149, 1979.
14. L. Tsai and Joshi, S., "Kinematics and optimization of a spatial 3-UPU parallel manipulator," *ASME Journal of Mechanical Design*, Vol. 122, No. 4, pp. 439-446 (2000).
15. J. A. Carretero, R. P. Podhorodeski, and M. A. Nahon., "Kinematic analysis and optimization of a new three degree-of-freedom spatial parallel manipulator," *ASME Journal of Mechanical Design*, Vol. 122, No. 1, pp. 17-24 (2000).
16. B. Hong and A.G. Erdman, "A method for adjustable planar and spherical four-bar linkage synthesis," *ASME Journal of Mechanical Design*, Vol. 127, No. 3, pp. 456-463 (2005).
17. M. Arsenault and R. Boudreau, "Synthesis of planar parallel mechanisms while considering workspace, dexterity, stiffness and singularity avoidance," *ASME Journal of Mechanical Design*, Vol. 128, No. 1, pp. 69-78 (2006).
18. A. A. Smaili, N. A. Diab, and N. A. Atallah, "Optimum synthesis of mechanisms using tabu-gradient search algorithm," *ASME Journal of Mechanical Design*, Vol. 125, No. 5, pp. 917-923 (2005).
19. G. N. Sandor and A. G. Erdman, "Advanced Mechanism Design Analysis and Synthesis," Prentice-Hall, Englewood Cliffs, 1984.
20. C. H. Suh and C. W. Radcliffe, "Kinematics and Mechanism Design," John Wiley and Sons, New York, 1978.
21. P. J. Martin, "Burmester Curve and Numerical Motion Generation of Grashof Mechanisms with Perimeter and Transmission Angle Optimization in MathCAD," Masters Thesis, New Jersey Institute of Technology, 2007.
22. R. L. Norton, "Design of Machinery 3<sup>rd</sup> Edition," McGraw Hill, New York, 2004.

## APPENDIX

**A1. The MathCAD commands in this section calculates all mechanism solutions for a given circle and center point curve**

$i := j := 0, 1, 2, \dots, \text{end} - 1$

$$\text{CRANK}_i := \text{FOLLOWER}_i := \sqrt{(\text{mx}_i - \text{kx}_i)^2 + (\text{my}_i - \text{ky}_i)^2}$$

$$\text{GROUND}_{i,j} := \sqrt{(\text{mx}_i - \text{mx}_j)^2 + (\text{my}_i - \text{my}_j)^2}$$

$$\text{COUPLER}_{i,j} := \sqrt{(\text{kx}_i - \text{kx}_j)^2 + (\text{ky}_i - \text{ky}_j)^2}$$

**A2. The MathCAD commands in this section select all mechanism solutions from among the solutions produced in Appendix A1 with feasible transmission angles**

```

START := 0          | STEP := 10          | END := 360

ANGLE := | for i ∈ 0..rows(COUPLER) - 1
          |   for j ∈ 0..rows(COUPLER) - 1
          |     
$$u_i \leftarrow \begin{cases} \frac{mx_i - kx_i}{\sqrt{(kx_i - mx_i)^2 + (ky_i - my_i)^2}} \\ \frac{my_i - ky_i}{\sqrt{(kx_i - mx_i)^2 + (ky_i - my_i)^2}} \end{cases} \text{ if } i \neq j$$

          |     
$$v_j \leftarrow \begin{cases} \frac{mx_j - mx_i}{\sqrt{(mx_j - mx_i)^2 + (my_j - my_i)^2}} \\ \frac{my_j - my_i}{\sqrt{(mx_j - mx_i)^2 + (my_j - my_i)^2}} \end{cases} \text{ if } i \neq j$$

          |     
$$\text{ANGLES}_{i,j} \leftarrow a \cos \left( \frac{u_i \cdot v_j}{|u_i| \cdot |v_j|} \right) \text{ if } i \neq j$$

          |     
$$\text{ANGLES}_{i,j} \leftarrow 0 \text{ otherwise}$$

          |   var_1 ← 0
          |   for i ∈ 0..rows(COUPLER) - 1
          |     for j ∈ 0..rows(COUPLER) - 1
          |       for  $\delta \in \text{START}, \text{STEP} \cdot \left( \frac{\pi}{180} \right) .. \text{END} \cdot \left( \frac{\pi}{180} \right)$ 
          |         
$$L \leftarrow (\text{GROUND}_{i,j})^2 + (\text{CRANK}_i)^2 -$$

          |         
$$(2 \cdot \text{GROUND}_{i,j} \cdot \text{CRANK}_i \cdot \cos(\text{ANGLES}_{i,j} + \delta))$$

          |         
$$\text{trans} \leftarrow a \cos \left[ \frac{(\text{COUPLER}_{i,j})^2 + (\text{FOLLOWER}_j)^2 - (L)}{2 \cdot \text{COUPLER}_{i,j} \cdot \text{FOLLOWER}_j} \right] \text{ if } i \neq j$$

          |         
$$\text{trans} \leftarrow 0 \text{ otherwise}$$

          |         var_1 ← augment(var_1, trans)
          |     ccolumns ← 1 +  $\left( \frac{\text{END}}{\text{STEP}} \right)$ 
          |     rrows ← cols(COUPLER)2
          |     M ← var_10,1
          |     for i ∈ 2..ccolumns
          |       M ← stack(M, var_10,i)
          |     for i ∈ 1..rrows - 1

```

```

Z ← var_1_{0,ccolumns-i+1}
for j ∈ 2..ccolumns
    Z ← stack(Z, var_1_{0,ccolumns-i+j})
M ← augment(M, Z)
M ← MT
for i ∈ 0, 1..  $\left(\frac{\text{cols}(\text{var}_1) - 1}{\text{ccolumns}}\right) - 1$ 
    for j ∈ 0, 1..  $\frac{\text{END}}{\text{STEP}}$ 
        Pi,j ← Mi,j
        Pi,0 ← 0 if  $\text{Re}(M_{i,j}) < \left(40 \cdot \frac{\pi}{180}\right) \vee \text{Re}(M_{i,j}) > \left(140 \cdot \frac{\pi}{180}\right)$ 
        Pi,j ← Mi,j otherwise
array ← (0 0 0 0)
array_1 ← (0 0 0 0)
for z ∈ 0..rows(P) - 1
    for i ∈ 0..rows(COUPLER) - 1
        for j ∈ 0..rows(FOLLOWER) - 1
            for δ ∈ 0
                if COUPLERi,j ≠ 0 ∧ FOLLOWERj ≠ 0
                    dummy ← a cos  $\frac{\left[ \begin{array}{l} (\text{COUPLER}_{i,j})^2 + (\text{FOLLOWER}_j)^2 - \\ (\text{GROUND}_{i,j})^2 + (\text{CRANK}_i)^2 - \\ (2 \cdot \text{GROUND}_{i,j} \cdot \text{CRANK}_i \cdot \\ \cos(\text{ANGLES}_{i,j} + \delta)) \end{array} \right]}{2 \cdot \text{COUPLER}_{i,j} \cdot \text{FOLLOWER}_j}$ 
                    array ← augment  $\begin{pmatrix} \text{CRANK}_i, \text{COUPLER}_{i,j}, \text{FOLLOWER}_j, \\ \text{GROUND}_{i,j} \end{pmatrix}$ 
                    if dummy = Pz,0
                        array_1 ← stack(array_1, array) if dummy = Pz,0
                    continue otherwise
array_1

```



| solution ← augment(M2,perimeter)

**A5. The MathCAD® commands in this section select the fixed and moving pivot coordinates of the solution produced in Appendix A4**

```
Cell3 := | for i ∈ 0..rows(kx) - 1
          |   Dummy_Follower ←  $\sqrt{(mx_i - kx_i)^2 + (my_i - ky_i)^2}$ 
          |   array ← augment(mx_i, kx_i, my_i, ky_i)
          |   coordinates ← array if Dummy_Follower = Cell20,0
          |   coordinates_1 ← array if Dummy_Follower = Cell20,2
          |   continue otherwise
          | solution ← stack(coordinates, coordinates_1)
```